J. Electr. Electron. Mater.
Vol. 38, No. 5, pp. 481-498 September 2025
doi: https://doi.org/10.4313/JEEM.2025.38.5.3
ISSN 1226-7945(Print), 2288-3258(Online)

Tutorial Status Report

리트벨트 정련법을 활용한 상전이 및 상분율 분석

심광보, 무하마드 시라즈, 김환민, 조성래, 안창원

울산대학교 반도체학과 및 에너지 하베스트-스토리지 연구소

초록: Rietveld refinement는 X선 회절 데이터를 이용한 다결정 시스템의 결정 구조 정량 분석에 필수적인 도구로 자리 잡았다. 본 튜토리얼 논문은 Rietveld refinement의 배경, 적용 사례 연구, 그리고 오픈 소스 소프트웨어 PROFEX를 활용한 실습에 중점을 두고 작성되었다. 격자 상수, 상분율과 같은 주요 구조적 매개변수는 전체 패턴 피팅을 통해 정량적으로 추출할 수 있다. 조성 변화, 전기장, 온도 변화, 그리고 배터리 사이클에 따른 상전이를 보여주는 사례 연구를 통한 재료 과학, 에너지 저장, 그리고 촉매 분야에서 Rietveld refinement의 유용성을 강조하고자 한다. 본 튜토리얼 논문에서는 Rietveld refinement 수행 절차를 $Bi_{1/2}Na_{1/2}TiO_3$ 페로브스카이트 세라믹을 예로 들어서 소프트웨어 설치, 결정구조 정보 파일 준비, Rietveld refinement 수행 단계, R 인자와 χ^2 값을 이용한 결과 평가, 그리고 수행 결과에 대한 정리에 대한 지침을 제공한다. 본 튜토리얼은 복잡한 재료 시스템에서 구조와 기능의 상관관계를 규명하고자 하는 연구자들을 위해 Rietveld refinement에 대한 이해 및 사용을 용이하게 하는 것을 목표로 한다.

키워드: Rietveld refinement, X-선 회절, 상전이 분석, 상분율

Phase Transition and Phase Fraction Analysis Using Rietveld Refinement

Gwangbo Sim, Muhammad Sheeraz, Hwan Min Kim, Sung-Lae Cho, and Chang Won Ahn

Department of Semiconductor Physics and Energy Harvest-Storage Research Center (EHSRC),
University of Ulsan, Ulsan 44610, Republic of Korea

(Received July 7, 2025; Revised August 7, 2025; Accepted August 11, 2025)

Abstract: Rietveld refinement has become an essential tool for the quantitative analysis of crystal structures in polycrystalline systems using X-ray diffraction data. This tutorial paper focuses on the background, case studies, and practical implementation of Rietveld refinement using the open-source software PROFEX. Key structural parameters, such as lattice constants and phase fractions, can be quantitatively extracted through full-pattern fitting. Case studies involving compositional variation, electric fields, temperature changes, and battery cycling demonstrate the broad applicability of Rietveld refinement in materials science, energy storage, and catalysis. A step-by-step procedure for performing Rietveld refinement is presented using $Bi_{1/2}Na_{1/2}TiO_3$ perovskite ceramic as an example, providing guidance on software installation, preparing crystal structure information files, performing Rietveld refinement, evaluating results using R-factor and χ^2 values, and summarizing the results. This tutorial aims to improve understanding and accessibility of Rietveld refinement for researchers seeking to investigate structure–property relationships in complex material systems.

Keywords: Rietveld refinement, X-ray diffraction, Phase transition analysis, Phase fraction

✉ **Chang Won Ahn; cwahn@ulsan.ac.kr**

G. Sim and M. Sheeraz contributed equally to this work.

1. INTRODUCTION

- X-ray diffraction (XRD) is one of the most widely used analytical techniques for characterizing the crystal structures of solid materials. It provides essential information, such as lattice parameters and crystal phases, thereby playing a critical role in materials science research, including new material development and the investigation of structure–property relationships.
- Traditional XRD analysis has primarily been limited to qualitative evaluations, such as phase identification and lattice parameter estimation based on the positions and intensities of diffraction peaks. However, the growing demand for quantitative analysis in complex systems, such as multi-phase materials, lattice distortion studies, and microstructural investigations, has highlighted the need for more advanced analytical techniques [1-3].
- Rietveld refinement is a powerful method that mathematically optimizes structural parameters by iteratively comparing the calculated diffraction pattern with the experimentally measured full-profile pattern. This technique enables the quantitative extraction of various crystallographic parameters, including lattice constants, atomic positions, thermal vibration factors, and phase fractions [4].
- In particular, Rietveld refinement is highly effective in quantifying phase fractions in multi-phase samples and identifying microstructural changes induced by doping, alloying, or thermal treatments. As a result, it is widely utilized across various fields, including materials science, solid-state physics, and energy-related materials research.
- This tutorial paper aims to introduce the application of Rietveld refinement for quantitative analysis of phase transitions and phase fractions using XRD data. Among the various software tools available for Rietveld refinement, we demonstrate the use of PROFEX (https://www.profex-xrd.org), an open-source platform, to analyze phase composition in multi-phase systems.

2. INTRODUCTION TO RIETVELD REFINEMENT

- XRD is a representative technique for analyzing crystal structures, based on the phenomenon of diffraction that arises from the periodic arrangement of atoms within a crystal lattice. According to Bragg's Law ($n\lambda = 2d\sin\theta$), constructive interference occurs when X-rays are diffracted by lattice planes with specific interplanar spacings, resulting in the formation of characteristic Bragg's diffraction peaks.
- The diffraction pattern serves as a fingerprint of the crystal structure of the sample. The θ-2θ scans positions of the diffraction peaks are closely related to the lattice parameters, while the intensities are influenced by atomic arrangement and structure factors. Consequently, XRD plays an important role in elucidating the crystal structures of the complex materials.
- Traditional XRD analysis typically involves identifying individual peaks to determine lattice parameters or to perform qualitative phase identification. However, such methods encounter significant limitations when analyzing structurally complex materials. To overcome these challenges and enable a comprehensive, quantitative interpretation of the entire diffraction pattern, the Rietveld refinement method is employed.
- Rietveld refinement was first introduced by Hugo Rietveld in 1969, originally developed for the analysis of neutron diffraction data. Since then, it has been successfully applied to XRD data and is now widely used for analyzing complex structures and multi-phase materials [4].
- The method was based on minimizing the difference between the observed and calculated diffraction patterns using a non-linear least-squares fitting approach. Starting from an initial structural model, the refinement process repeatedly adjusted various parameters, such as lattice constants, atomic positions, and thermal vibration factors, to minimize the discrepancy between the experimental and simulated patterns.
- Unlike conventional qualitative methods that focus solely on individual peak positions or intensities, Rietveld refinement utilizes the entire diffraction profile. This enables the extraction of a broader range of structural information with higher accuracy. It is particularly powerful for the quantitative analysis of multi-phase mixtures [5].

3. INFORMATION OBTAINABLE FROM RIETVELD REFINEMENT

- Crystal Structure and Lattice Constants
  - Rietveld refinement enables the quantitative determination of crystal structures, including space group symmetry, atomic arrangements, and lattice parameters (a, b, c, α, β, γ). It is also effective for tracking changes in lattice constants resulting from substitution, doping, thermal expansion, or phase transitions.
- Phase Fractions
  - When multiple crystalline phases are present in a diffraction pattern, their relative abundances can be quantitatively estimated. This allows for the detection of phase transitions induced by processes, such as heat treatment or the application of electric fields. The method is particularly useful for systematic compositional analysis of complex multi-phase systems.
- Crystallographic Orientation (Preferred Orientation)
  - The degree of preferred orientation, where crystals grow preferentially along specific directions, can be evaluated through refinement. This analysis is also applicable to various processes, such as tape casting and spark plasma sintering. Furthermore, understanding crystallographic orientation provides insight into the anisotropic behavior of materials.

4. CASE STUDIES OF PHASE TRANSITION ANALYSIS USING RIETVELD REFINEMENT

- The structural characteristics of materials often undergo various phase transitions and lattice distortions in response to changes in external environments. Factors such as compositional variation, application of electric fields or mechanical pressure, thermal treatment, gas atmosphere, and light irradiation can alter the ionic arrangement, bond lengths, and symmetry within the crystal structure. These changes are typically reflected in the diffraction pattern.
- This section presents representative case studies in which Rietveld refinement is employed to analyze phase transitions caused by compositional modification, external stimuli (such as electric fields and temperature), and chemically induced lattice transformations [6-13].

4.1 Phase Fraction Analysis According to Compositional Variation

- Phase evolution in $(0.935–x)Bi_{1/2}Na_{1/2}TiO_3–0.065BaTiO_3–xBi(Mn_{1/2}Ce_{1/2})O_3$ ceramics
  - N. Ullah Khan *et al*. investigated the incorporation of

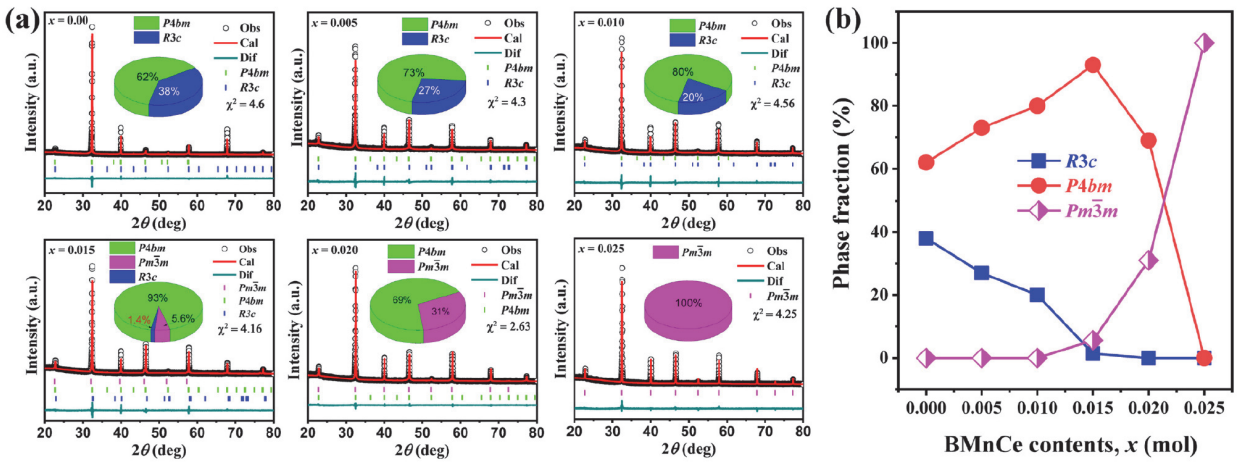

Fig. 1. (a) Rietveld refinement results for poled $(0.935-x)Bi_{1/2}Na_{1/2}TiO_3$-$0.065BaTiO_3$-$xBi(Mn_{1/2}Ce_{1/2})O_3$ ceramics using $R3c$, $P4bm$, and $Pm\bar{3}m$ phases. The inset shows the phase fraction of rhombohedral ($R3c$), tetragonal ($P4bm$), and cubic ($Pm\bar{3}m$) phases and (b) phase fraction of rhombohedral ($R3c$), tetragonal ($P4bm$), and cubic ($Pm\bar{3}m$) phase as a function of BiMnCe content. Adapted with permission from [14]. Copyright 2024 Elsevier.

$Bi(Mn_{1/2}Ce_{1/2})O_3$ (BMnCe) as a solid solution into the $Bi_{1/2}Na_{1/2}TiO_3$-$BaTiO_3$ (BNT–BT) system to enhance its electrostrain performance (Figs. 1(a) and (b)) [14]. Their study revealed that the addition of BiMnCe lowers the ferroelectric-to-relaxor phase transition temperature ($T_{F–R}$) below room temperature and promotes the stabilization of the ergodic relaxor (ER) phase. Rietveld refinement analysis demonstrated a gradual structural evolution with increasing BiMnCe content, from a coexisting rhombohedral (*R*3*c*) and tetragonal (*P*4*bm*) phase toward a predominantly tetragonal structure, and eventually to a pseudocubic ($Pm\bar{3}m$) symmetry. These structural changes were quantitatively analyzed through phase fraction and lattice parameter evaluations using XRD, providing systematic insight into the mechanisms underpinning ER phase stabilization.

- Based on this structural analysis, the composition (0.935-*x*)BNT-0.065BT-*x*BMnCe with $x = 0.01$ exhibited an optimal electrostrain of 0.43%, a normalized strain (S_{max}/E_{max}) of 716 pm/V, an electrostrictive coefficient $Q_{33} = 0.032$ m^4/C^2, and a $Q_{33}/E = 5.33\times10^{-9}$ m^5/C^2V. Note that the phase structure of (0.935-*x*)BNT-0.065BT-*x*BMnCe was observed to undergo a progressive evolution, initially exhibiting a coexistence of rhombohedral (*R*3*c*) and tetragonal (*P*4*bm*) phases, transitioning toward a dominant tetragonal (*P*4*bm*) phase with increasing BMnCe content, and eventually transforming into a pseudocubic phase at higher doping levels. The high electrostrain at $x = 0.01$ was accompanied by a notable structural transition to *P*4*bm* phase fraction from *R*3*c*, suggesting a strong correlation between phase structure and electromechanical response (Figs. 2(a) and (b)).
- Moreover, this composition demonstrated thermal stability up to 120°C, suggesting strong potential for high-temperature actuator applications. The study effectively established the quantitative relationship between structural phase evolution and functional performance via Rietveld refinement, validating the role of compositional tuning as a key strategy in designing high-performance lead-free BNT–BT-based ceramics.

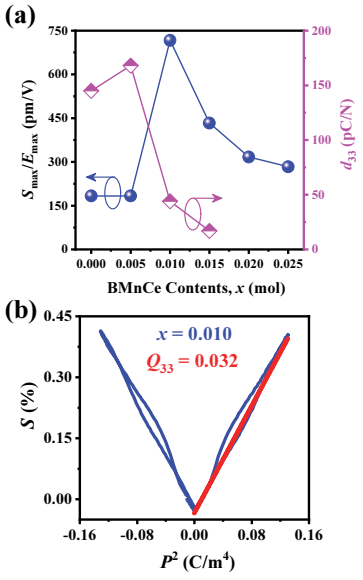

Fig. 2. (a) Normalized strain (S_{max}/E_{max}) and d_{33} values as a function of BMnCe content in (0.935-*x*)BNT-0.065BT-*x*BMnCe ceramics. For d_{33} measurements, we poled the sample at 4.5 kV/mm and (b) strain (S) vs. polarization square (P^2) plots of three representative compositions of (0.935-*x*)BNT-0.065BT-*x*BMnCe ceramics. Adapted with permission from [14]. Copyright 2024 Elsevier.

■ Phase structure in (1-*x*)$Bi_{1/2}Na_{1/2}TiO_3$-*x*$Bi(Li_{1/3}Zr_{2/3})O_3$ ceramics

- S. Ali *et al*. conducted Rietveld refinement analysis on (1-*x*)$Bi_{1/2}Na_{1/2}TiO_3$-*x*$Bi(Li_{1/3}Zr_{2/3})O_3$ (BNT-BLZ) ceramics. $Bi(Li_{1/2}Zr_{2/3})O_3$ (BLZ), which is a low-tolerance-factor end-member compound, was introduced as a solid solution into the lead-free $Bi_{1/2}Na_{1/2}TiO_3$ (BNT) matrix (Fig. 3) [5]. The analysis revealed the formation of a morphotropic phase boundary (MPB) within the composition range of $x = 0.01$–0.02, where a coexistence of rhombohedral (*R*3*c*) and tetragonal (*P*4*bm*) phases was quantitatively confirmed [8]. This structural feature was directly linked to enhanced electrical properties, including a high remanent polarization ($P_r \approx 34$ μC/cm^2) and a piezoelectric coefficient ($d_{33} \approx 107$ pC/N), illustrating a strong correlation between phase structure and electromechanical performance. The study further proposed an optimal tolerance factor range ($t = 0.9750$–0.9757) for MPB formation in BNT-based systems, offering valuable compositional design guidelines.

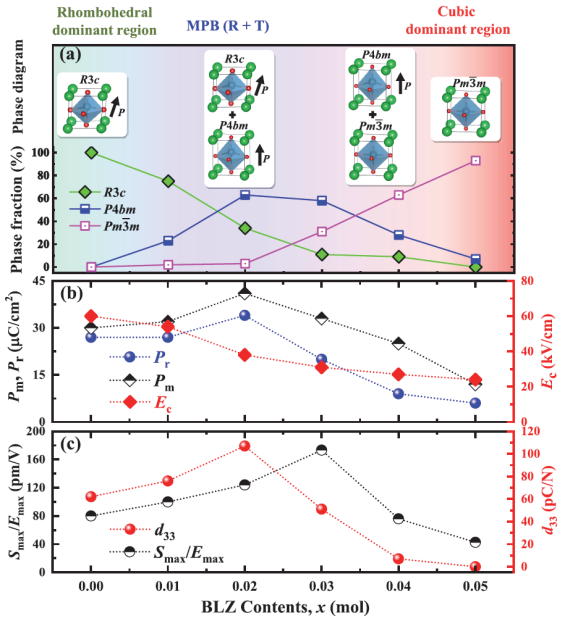

Fig. 3. Phase diagram of (1-*x*)$Bi_{1/2}Na_{1/2}TiO_3$-*x*$Bi(Li_{1/3}Zr_{2/3})O_3$ (BNT-BLZ) ceramics; (a) The percentage of phases as a function of BLZ content, (b) composition dependence of maximum polarization (P_m), remnant polarization (P_r), and coercive field (E_c) of BNT-BLZ samples, and (c) the variant trend of normalized strain (S_{max}/E_{max}) and piezoelectric coefficient (d_{33}) as a function of BLZ content. Adapted with permission from [8]. Copyright 2024 Elsevier.

4.2 Electric-Field-Induced Phase Transition Analysis

- M. Sheeraz *et al*. investigated the electric-field-induced electrostrain behavior of $Bi_{1/2}Na_{1/2}TiO_3$–$BiAlO_3$ (BNT–BA) ceramics using *in situ* XRD combined with Rietveld refinement using PROFEX, revealing that structural phase transitions under external electric fields played a decisive role in the electromechanical response (Fig. 4) [9]. Upon removal of the electric field, the material exhibited a coexistence of cubic and rhombohedral phases. When the electric field was applied, the structure transitioned to a mixture of rhombohedral and tetragonal phases, followed by a reversible transition back to the cubic–rhombohedral coexistence upon removal of the electric field.
- As a result, the BNT–BA thin film demonstrated a normalized electrostrain (S_{max}/E_{max}) of 203 pm/V and an effective transverse piezoelectric coefficient ($e_{31,f}$) of 2.48 C/m^2. This study provided a clear mechanistic

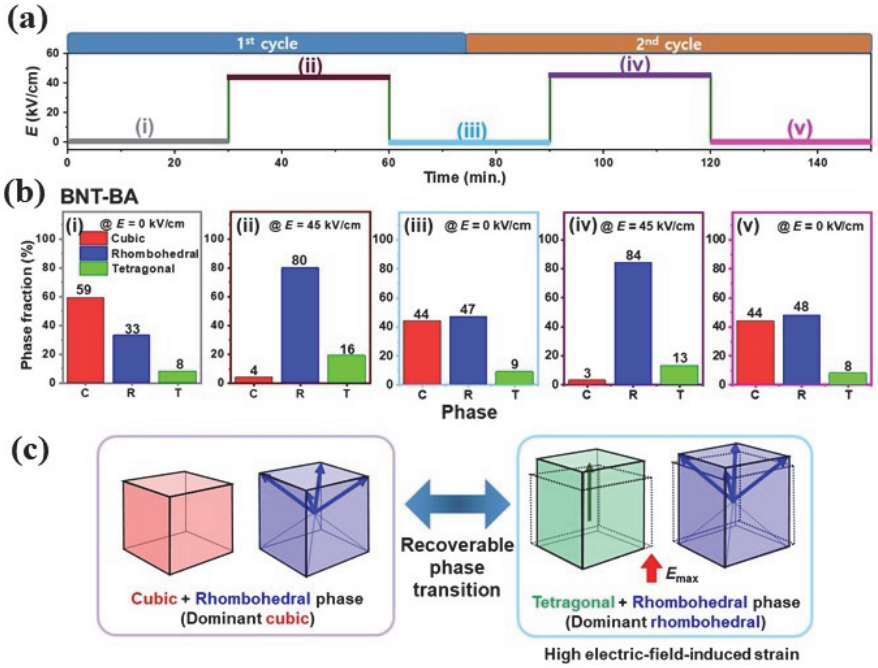

Fig. 4. (a) Electric-field-dependent *in situ* XRD performed in five steps, (b) phase fractions of each phase were derived from XRD Rietveld refinement of BNT–BA sample at the corresponding five steps. Phase fractions for cubic, rhombohedral, and tetragonal crystal symmetries at each step were represented by red, blue, and green blocks, respectively, and (c) schematic diagram of electric-field-induced structural changes in BNT–BA. Adapted with permission from [9]. Copyright 2025 Elsevier.

understanding of the electric-field-driven structural phase transitions in BNT-based thin films through real-time quantitative analysis. The findings were a step towards the rational design of high-performance lead-free actuator materials by elucidating the correlation between structure and electromechanical properties [6,15].

4.3 Structural Evolution During Charge–Discharge in Lithium-Ion Batteries

- The insertion and extraction of lithium ions induced changes in the oxidation state and bonding environment of transition metal ions within the electrode material. These changes led to variations in interlayer spacing (particularly along the *c*-axis) and bond angles, which resulted in irreversible structural transformations or the emergence of new phases during electrochemical cycling.
- L. de Biasi *et al*. investigated the phase transitions and stability issues of the $LiNiO_2$ (LNO) cathode material. Using operando XRD coupled with Rietveld refinement, the multi-step phase transitions were quantitatively analyzed that occur during charge–discharge processes (Fig. 5) [10]. During charging, LNO sequentially undergoes transitions through the H1 (hexagonal) → M (monoclinic) → H2 (hexagonal) → H3 (hexagonal) phases. Notably, the transition from H2 to H3 was accompanied by a sharp contraction of the *c*-axis lattice parameter, resulting in a 3.8% reduction in unit cell volume.
- This structural transfer generated internal mechanical stress, which contributed to particle cracking and irreversible degradation. These were major factors in the capacity fading of LNO cathodes. Through Rietveld refinement, the study tracked the lithium content range *x*(Li) for each phase, phase fractions, lattice parameter changes, and variations in Li–O and Ni–O bond distances. These detailed structural insights revealed a strong correlation between lattice instability and oxygen release, providing critical understanding of the intrinsic factors limiting the long-term stability of layered oxide cathodes.

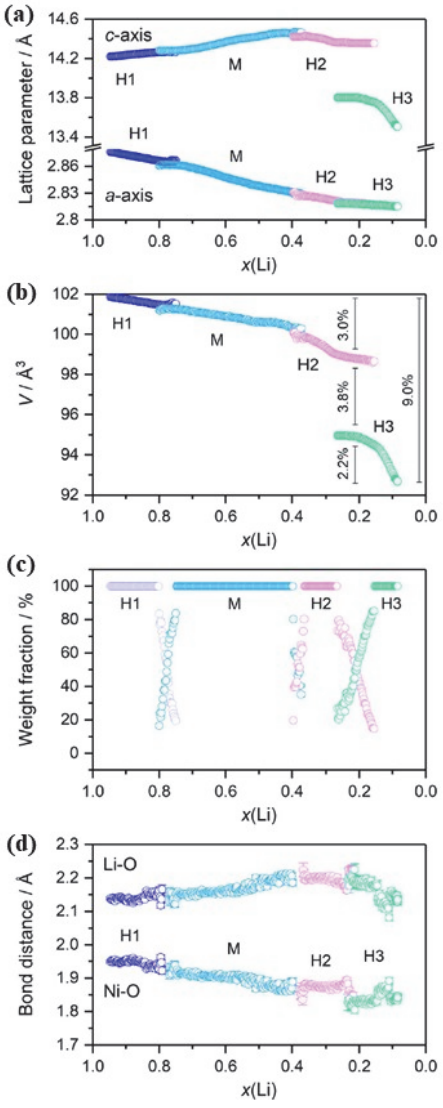

Fig. 5. Results from Rietveld refinement analysis of operando XRD data obtained for a Li/LNO cell. (a) Evolution of the *a*- and *c*-lattice parameters, (b) unit-cell volume, (c) weight fractions, and (d) Li-O and Ni-O bond distances for the different Li_xNiO_2 phases in the 2nd charge cycle. Adapted with permission from [10]. Copyright 2019 Wiley.

4.4 Temperature-Induced Phase Transitions

- As temperature increases, ferroelectric materials typically lose their spontaneous polarization at the Curie temperature (T_c), undergoing a phase transition to a centrosymmetric cubic structure. Such transitions can be identified in XRD patterns through the convergence of lattice parameters, the merging or splitting of characteristic peaks, and an increase in thermal vibration factors.

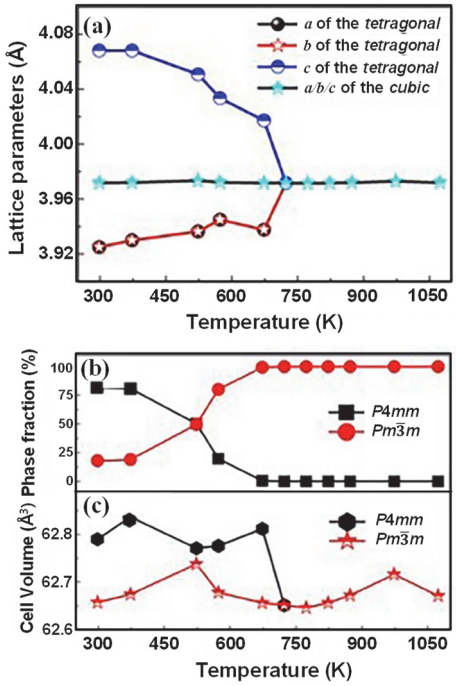

Fig. 6. (a) Lattice parameters, (b) phase fraction, and (c) unit cell volume changes with temperature. Adapted with permission from [11]. Copyright 2024 The American Ceramic Society.

- K. Chen *et al*. investigated the temperature-dependent phase transitions of $0.55Bi(Mg_{1/2}Ti_{1/2})O_3$–$0.45PbTiO_3$ ceramics to evaluate their high-temperature piezoelectric stability (Fig. 6) [11]. Based on the XRD results, Rietveld refinement analysis revealed a coexistence of tetragonal (*P*4*mm*) and pseudo-cubic ($Pm\bar{3}m$) phases. Over the temperature range of 293–733 K, the persistence of peak splitting between the (002) and (200) reflections, along with continuous changes in lattice parameters, confirmed the thermal stability of the tetragonal phase.
- A distinct ferro-to-paraelectric phase transition was observed at a temperature of 733 K, where the tetragonal phase fully disappeared, and a complete transformation to the cubic structure occurred. The quantitative analysis of phase fractions and unit cell volume across temperatures provided critical insights into the local structural dynamics, which were directly linked to the material's electrical properties. These structural findings emphasized the importance of lattice stability for the reliable performance of piezoelectric ceramics under thermal stress.

4.5 Lattice Distortion Analysis of Catalysts During Chemical Reactions

- In catalytic or electrochemical materials, chemical reactions could induce structural changes within the crystal lattice, including modifications in local bonding environments, ionic arrangements, and overall lattice geometry. These reaction-induced effects result in lattice expansion, symmetry changes, or the formation of new phases. Rietveld refinement served as a powerful tool for quantitatively analyzing such structural variations.
- J. Goetze *et al.* examined the lattice expansion behavior of small-pore zeolite catalysts (specifically CHA, DDR, and LEV frameworks) during the methanol-to-olefins (MTO) reaction. By combining operando XRD with UV–vis spectroscopy, it was investigated how the accumulation of organic species quantitatively affects the zeolite crystal structures [13]. Rietveld refinement of the XRD patterns before and after reaction revealed that the SSZ-13 catalyst with CHA structure exhibited a significant *c*-axis lattice expansion of up to 0.9%. This expansion was attributed to the retention of aromatic species such as methylated naphthalene and pyrene within the zeolite framework.
- This study presents a representative example in which Rietveld analysis was used to confirm that catalyst deactivation during MTO reactions was structurally linked to the accumulation of coke-like species within the lattice, highlighting the utility of crystallographic refinement for probing reaction-induced degradation mechanisms at the atomic scale.

5. RIETVELD REFINEMENT WORKFLOW AND PRACTICAL PROCEDURE

5.1 Software Installation and Reference Structure File Preparation

- This section outlines the step-by-step procedure for performing Rietveld refinement using real XRD data with the PROFEX software.
- PROFEX is an open-source graphical user interface for the BGMN Rietveld refinement engine and can be freely downloaded from the official website: https://www.profex-xrd.org.

- The hands-on practice in this tutorial is based on a perovskite ceramic material. The pure $Bi_{1/2}Na_{1/2}TiO_3$ (BNT) system is used as an example for understanding the Rietveld refinement using PROFEX.
- Crystallographic Information Files (CIF, file extension : **.cif), which represent the reference files required for Rietveld refinement, can be obtained from databases such as the Materials Project (https://next-gen.materialsproject.org) or the Crystallography Open Database (COD) (https://www.crystallography.net). In this study, most of the structure files were retrieved from COD.

5.2 Importing XRD Data

- After launching PROFEX, the measured XRD data can be imported by selecting **File** > **Open Raw Data Files** from the top menu (Fig. 7(a)).
- In our case, we selected the file with a name of "pure BNT E-0.xy" highlighted with a light blue color in Fig. 7(b). The XRD data of the BNT sample was collected using the lab source Brucker XRD machine.
- Once the CIF files are uploaded, the diffraction data will be visualized in a graph format, and the dataset will automatically appear in the list on the left-hand side of the window (Fig. 7(c)).

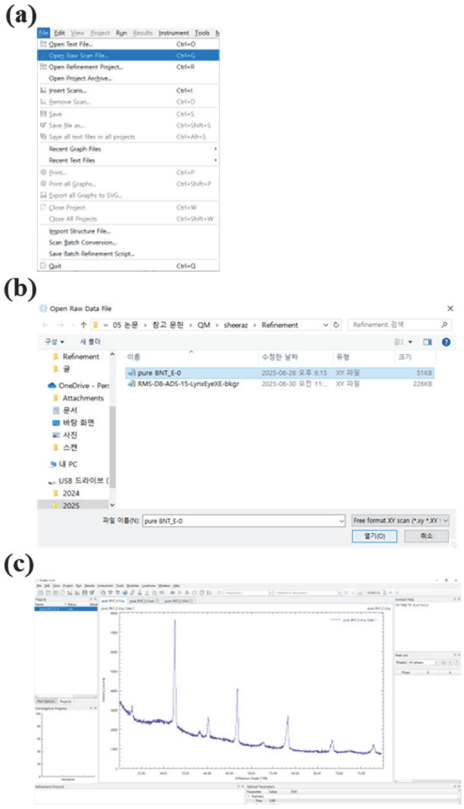

Fig. 7. (a-c) Screen capture of the steps for importing XRD data into the PROFEX program.

5.3 Loading and Converting Reference Structure Files

- To load the crystal structure data, navigate to **File** > **Import Structure Files** (Fig. 8(a), (b)), and then select the desired Crystallographic Information Files (CIF, **.cif) using the **Load Source Files** function (Fig. 8(c), (d)).

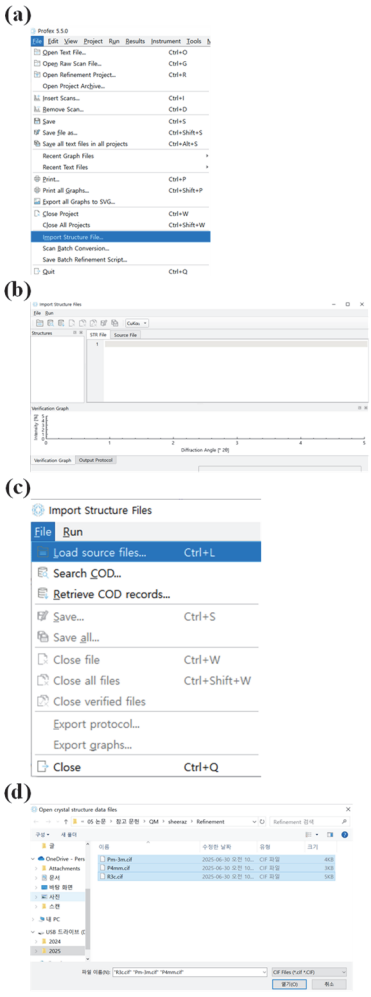

Fig. 8. (a-d) Screen capture of the steps for loading of Crystallographic Information Files (CIF, file extension : .cif) and converting to STR (file extension : **.str) file.

- Upon loading, the selected CIF file automatically changes to a STR file (file extension : **.str) containing a structural model for a crystalline material, as represented by a black rectangle in Fig. 9(a). This STR file defines the crystal structure, including the unit cell parameters, atomic positions, and thermal parameters. It serves as the starting point for the Rietveld refinement process, where a calculated diffraction pattern based on this model is iteratively adjusted to match the experimentally observed diffraction pattern.
- The STR file can be verified by selecting **Run** > **Verify Structure**, which checks for syntax or logical errors in the structure definition (Fig. 9(b)). If no errors are found, a preview of the calculated peak positions will be displayed at the bottom of the window, which is highlighted with a black rectangle in Fig. 9(c).

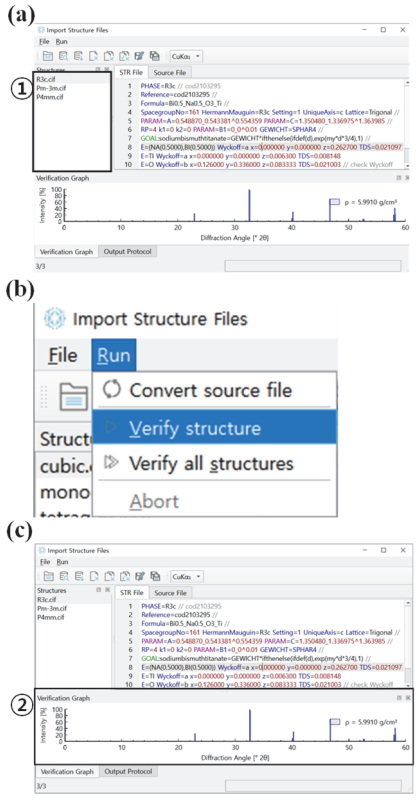

Fig. 9. (a-c) Screenshot illustrates the verification steps of the reference CIF file used in the Rietveld refinement process. After loading Crystallographic Information Files (Fig. 8.), selected data appeared on the left-hand side of the window, represented by a vertical black rectangle ①. After verifying the STR files, the calculated XRD pattern will appear at the bottom side of the window, shown by a horizontal rectangle ②.

- Once verified, save the STR file using the save icon at the top of the window in a folder with specific names and close the **Import Structure Files** dialog (Fig. 10(a), (b)).
- In case of BNT, we saved a rhombohedral phase with *R*3*c*, a tetragonal phase with *P*4*mm*, and a cubic phase with a name $Pm\bar{3}m$ (Fig. 10(c)).

5.4 Applying Structure and Instrument Configuration to Experimental Data

- To apply the structure file to the experimental dataset, click the "±" icon (shown by a red square in Fig. 11 (a)) located in the upper-left corner of the PROFEX interface to open the **Add/Remove Phases** window. From here, select the desired STR file for Rietveld refinement, as shown in Fig. 11(b).
- Next, choose an XRD instrument model that closely resembles the one used in the measurement. This automatically applies relevant instrument parameters, such as X-ray wavelength, 2θ range, and instrument broadening parameters (selected with the blue color in Fig. 11(c)).

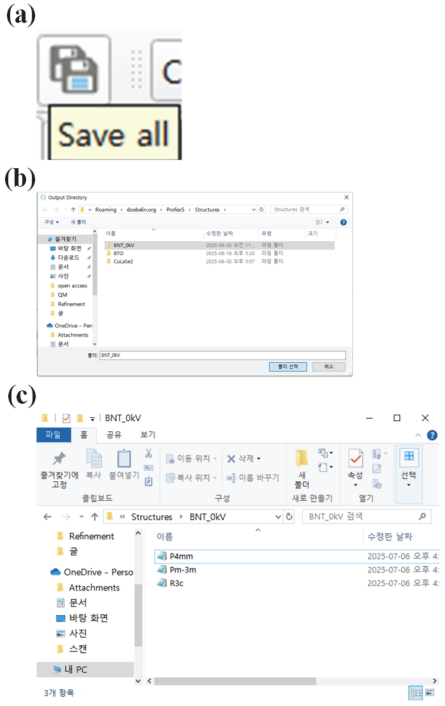

Fig. 10. Screenshot illustrates how to save the verified CIF files using the PROFEX. (a) Click the Save all icon and (b) select the save folder, (c) the STR file is saved on "C:\Users\[Username]\AppData \Roaming\doebelin.org\Profex5\Structures\[Filename]".

- For more detailed instrument configuration, go to **Instrument** > **Edit Current Configuration**, where settings related to the primary beam, sample stage, and secondary optics can be customized (Fig. 12(a), (b)).
- Once both the structure and instrument settings are completed, the finalized STR file is generated (Fig. 13(a)).
- The initially generated STR file contains fixed constant values (imported from the CIF file). Before performing refinement, these fixed constant values must be converted into variable ranges that can be adjusted during the refinement process.
- For example, in the initially generated *R*3*c*.str file, the value may appear as a fixed entry such as “C=1.350480”. When the user selects this parameter with the mouse pointer and right-clicks, a context menu appears, as shown in Fig. 13(b). By clicking **Refine parameter** in this menu, the fixed value “C=1.350480” is changed to a variable range format, such as “PARAM=C=1.350480_1.336975^1.363985”. This allows the lattice constant c to vary within the specified range during refinement to determine the most appropriate value.
- Conversely, a parameter can also be fixed again by reversing this process.

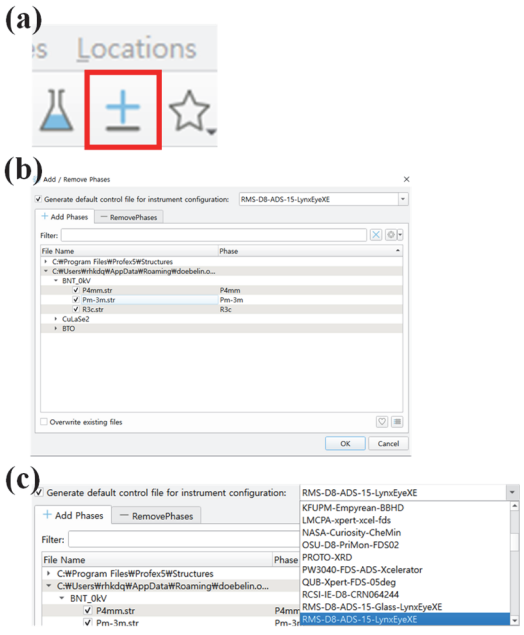

Fig. 11. (a-c) Screen capture of the steps for applying the structural (STR file) and instrumental configuration to experimental data in the PROFEX.

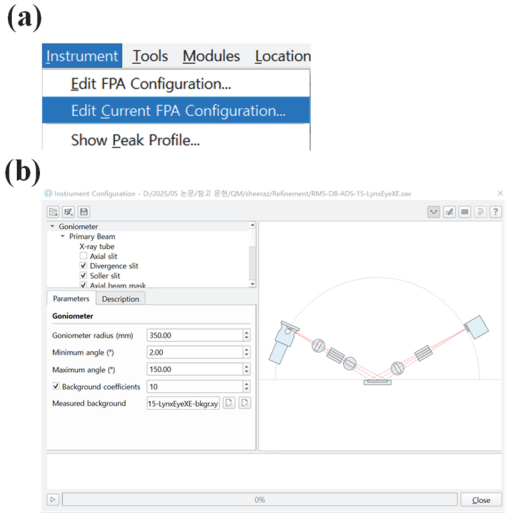

Fig. 12. (a, b) Screen capture of the steps to set up more detailed device configuration (X-ray tube, sample stage, secondary beam) using PROFEX.

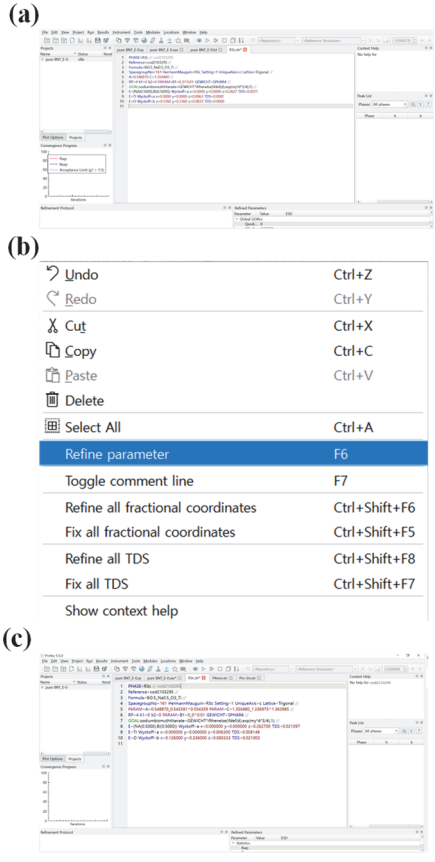

Fig. 13. (a-c) Figure showing the process of converting a fixed parameter into a refinable variable range in the STR file using the ‘Refine parameter’ option.

5.5 Procedure, Role, and Evaluation of Le Bail Refinement [16]

- Le Bail refinement is a whole-pattern fitting technique used to improve the agreement between observed and calculated X-ray diffraction patterns by refining peak positions and intensities based solely on the material's lattice parameters and space group, without the need for detailed atomic coordinates. Unlike Rietveld refinement, it does not require information such as atomic positions or thermal vibration factors. This method is particularly useful for verifying and adjusting initial lattice parameters and for analyzing multiphase samples. It is often employed as a preliminary step before performing full Rietveld refinement.
- In Profex, Le Bail refinement can be activated by adding the command "LeBail=1" to the STR file, as indicated by ① in Fig. 14. When this option is enabled, the refinement calculates peak positions and intensities based solely on the space group and lattice parameters, without considering atomic coordinates.
- Conversely, if "LeBail=0" is specified or the command is omitted entirely, the software performs a full Rietveld refinement, which requires a complete structural model including atomic positions.
- To perform the Le Bail refinement of the corresponding BNT XRD. Click the **Run the refinement** button represented by the "▷", and the Le Bail refinement process is initiated. The calculated diffraction pattern is iteratively compared to the experimental data, and various parameters are optimized through successive refinement cycles (Fig. 15 (a)).
- As the refinement proceeds, the χ^2 curve converges and the fit between the experimental and calculated patterns improves (Fig. 15 (b), (c)). However, the refinement quality of the XRD results should be assessed based on quantitative indicators rather than a separate visual inspection.
- Refinement Quality Indicators [17]
  - R_{wp} (Weighted-profile R-factor) represents the weighted average of the differences between the observed diffraction intensities and the calculated intensities, taking measurement errors into account. A lower R_{wp} value indicates better agreement between the calculated and experimental patterns. It reflects the overall quality of the pattern fit. Generally, values below 15% are considered indicative of a well-refined result.
  - R_{exp} (Expected R-factor) is the statistically expected minimum value of R_{wp}, based on the noise level and number of data points in the experimental dataset. When R_{wp} approaches R_{exp}, the refinement is statistically reliable. R_{exp} is used in conjunction with R_{wp} to calculate the chi-squared (χ^2) value, which is a key indicator of refinement quality.

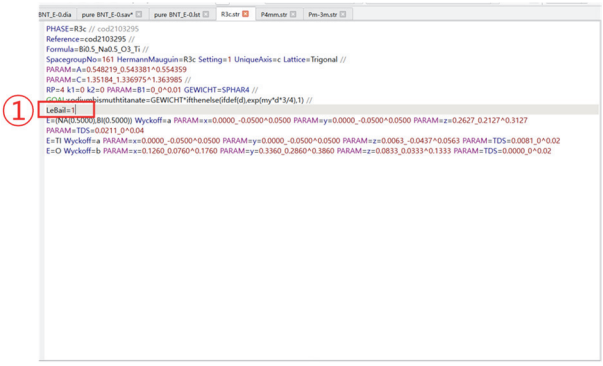

Fig. 14. Activation of Le Bail refinement by adding the command "LeBail=1" to the STR file.

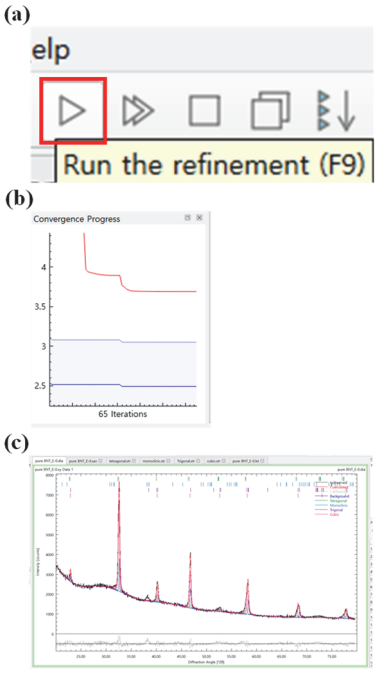

Fig. 15. (a-c) Screen capture of the steps for the initiation of the XRD fitting through the Le Bail refinement process.

- R_{phase} (Phase specific R-factor) is the R-factor calculated individually for each phase in a multiphase refinement. It reflects how well calculated pattern of a specific phase matches the corresponding portion of the observed data. A significantly higher R_{phase} compared to the overall R_{wp} may indicate issues in the selection of STR file or lattice constant of that phase, requiring further refinement or adjustment.
- χ^2 or GoF (Goodness of Fit) : The χ^2 (chi-squared) value, also referred to as the Goodness of Fit (GoF), as shown in Equation (1), is used to evaluate the reliability of the refinement. A value of $\chi^2 \approx 1$ is considered ideal; values between 1 and 2.5 are generally acceptable. Values above 3 suggest the need to revise or improve the structural model used in the refinement.

$$\text{GoF} = \frac{R_{wp}}{R_{exp}}, \quad \chi^2 = \left(\frac{R_{wp}}{R_{exp}}\right)^2 \qquad \text{Equation (1)}$$

- After the activation step, Le Bail refinement utilizes the specified space group and lattice parameters to calculate peak positions based on Bragg's law, while estimating peak intensities through the application of a peak profile function. This process generates the calculated diffraction pattern (Y_{cal}), represented by green box in Fig. 16.
- In the case of multiphase samples, Y_{cal} is separated into individual phase contributions, as demonstrated in Fig. 17. This can be achieved by comparing Y_{cal} with the observed diffraction pattern (Y_{obs}) and assigning weighted contributions to each phase based on the peak positions of their respective reference patterns, allowing for iterative estimation of each phase contribution.
- The refinement process iteratively minimizes the difference between Y_{obs} and Y_{cal} using a nonlinear least-squares algorithm. While structural parameters remain fixed, the refinement adjusts peak positions and intensities to achieve the best fit between the calculated and observed diffraction patterns, as presented in Fig. 18.

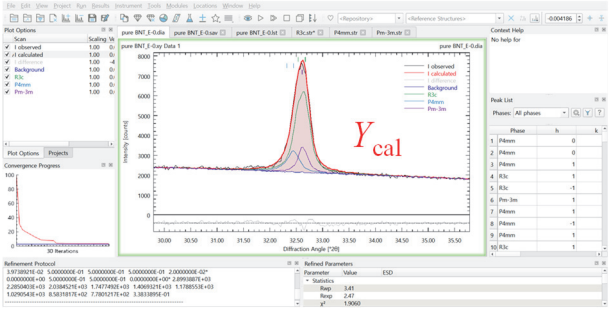

Fig. 16. Calculated diffraction patterns (Y_{cal}) based on lattice constants.

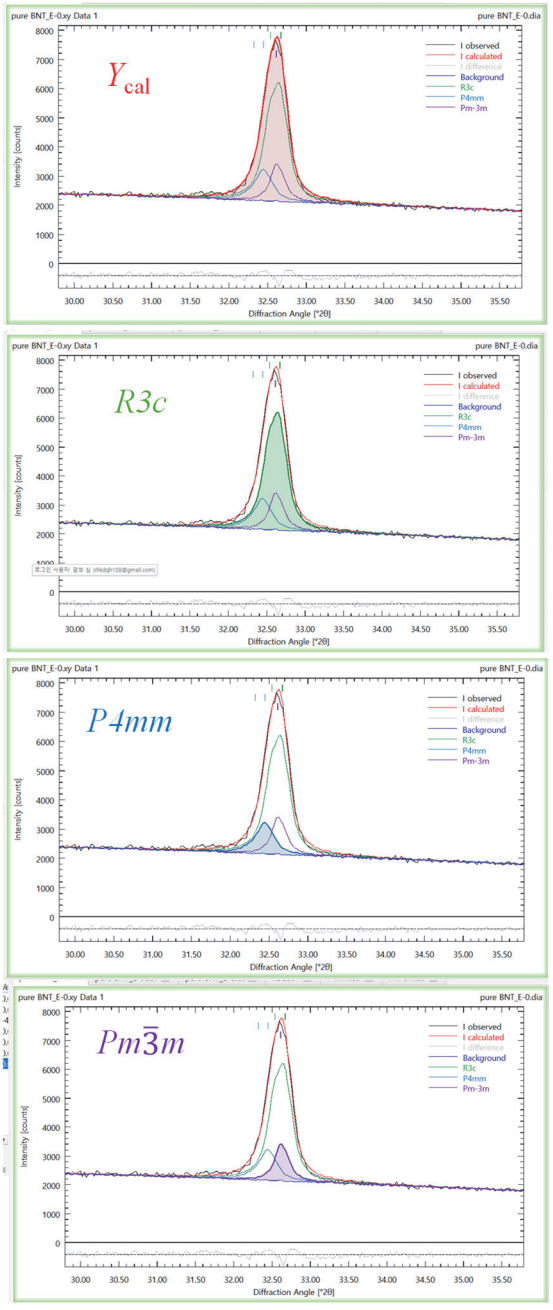

Fig. 17. Separation of Y_{cal} into phase-specific components for multiphase analysis.

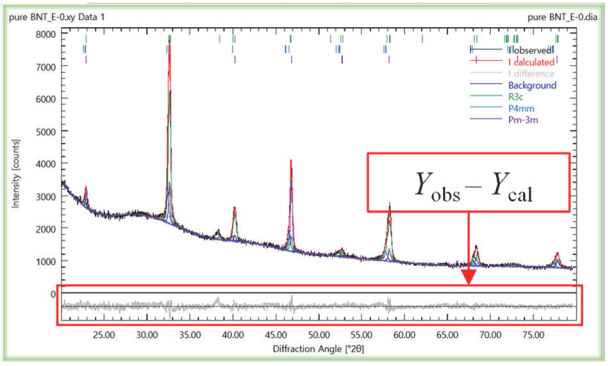

Fig. 18. Screen capture of the minimized difference between Y_{obs} and Y_{cal} after the refinement process.

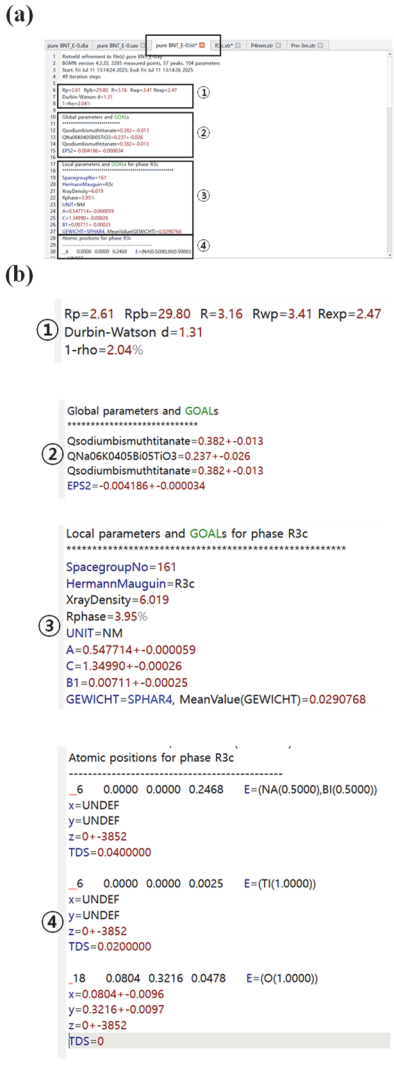

Fig. 19. (a) Screenshot of the "**.lst" file obtained after the refinement process and (b) enlarged information such as ① refinement indicator, ② phase fraction, ③ lattice constant, and ④ atomic positions.

- After the refinement process, the "**.lst" file provides detailed information including refinement indicator, phase fraction, lattice constant, and atomic positions as shown in Fig. 19.
- R_{phase} serves as a diagnostic tool for identifying problematic phases within the refinement (Fig. 20). If a certain phase shows significantly higher R_{phase} than others, it may suggest issues in the corresponding structure file, such as inaccurate lattice parameters or an inappropriate structural model in the corresponding structure file, requiring further modification or replacement, as presented in Fig. 21. These evaluation criteria and procedures (Fig. 20 and Fig. 21), particularly the use of R_{wp}, χ^2, and R_{phase}, are also equally applicable to the Rietveld refinement process.
- If the R-factor of the result obtained from Le Bail Refinement is 15 or more, or χ^2 is not within the range of 1 to 3.5, modify the lattice constant obtained from the "**.lst" file to the STR file and re-run Le Bail Refinement. This process can improve the goodness of fit of the refinement result (Fig. 21).
- If the goodness of fit of the refinement result does not improve despite repeating this process, replace the STR file with a different space group or lattice constant than the

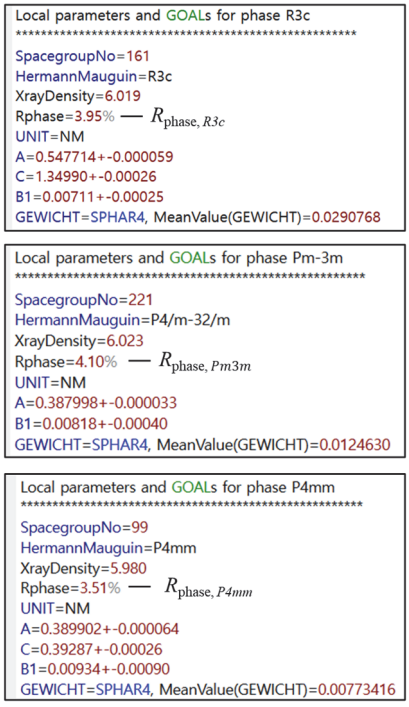

Fig. 20. Identification of problematic phases using R_{phase} values.

previously used STR file and run it again from the beginning.

- This stepwise approach is particularly effective for analyzing complex multiphase samples or cases where structural information is incomplete or uncertain. It significantly improves the reliability and efficiency of Rietveld refinement by enabling early detection and correction of structure mismatches.
- Once optimal fit is achieved according to the refinement quality indicator, the user can perform Rietveld refinement for full structural analysis after removing the "LeBail=1" command (Fig. 22).

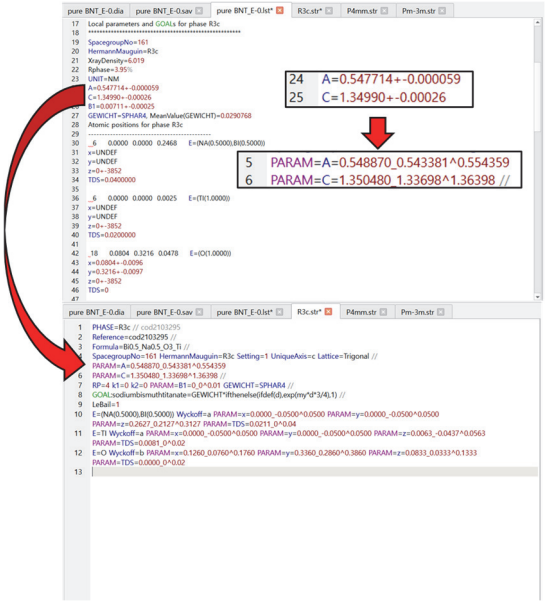

Fig. 21. Modification of STR files in the PROFEX program window based on Le Bail refinement results.

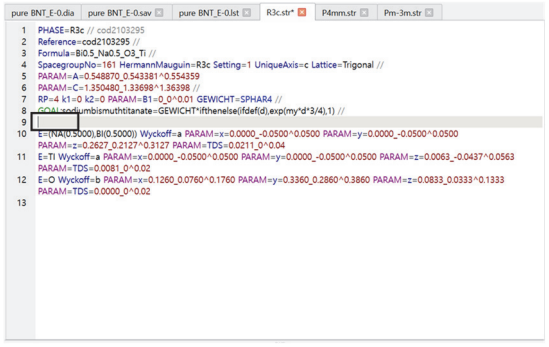

Fig. 22. Screenshot of an STR file with the "LeBail=1" command removed to perform Rietveld refinement.

5.6 Executing and Evaluating Rietveld Refinement

- After performing Le Bail Refinement, Rietveld refinement can be performed using the modified STR file. Click the Run button represented by the "▷" button (as shown in Fig. 15(a)), the Rietveld refinement process is initiated. The calculated diffraction pattern is iteratively compared to the experimental data, and various parameters are optimized through successive refinement cycles.
- Upon completion of the refinement, the resulting "**.lst" file contains detailed information, such as quality factor, phase fractions, and lattice parameters. If necessary, the STR file can be modified, and the refinement should be repeated to further improve the XRD fit (Fig. 23(a) and (b)).
- Once the refinement is completed, the results can be interpreted and evaluated using the output **.lst file and

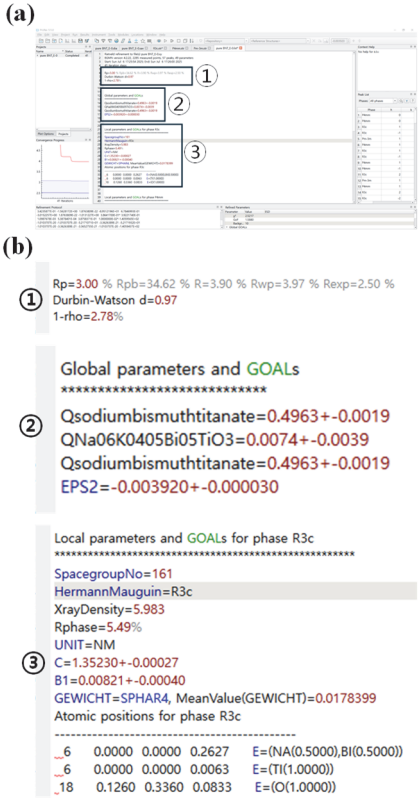

Fig. 23. (a) Screen capture of a window showing the results after performing the Rietveld refinement process and (b) the highlighted areas ①, ②, and ③ in (a) represent the refinement quality, phase fraction of each phase, and lattice parameters based on each phase, respectively.

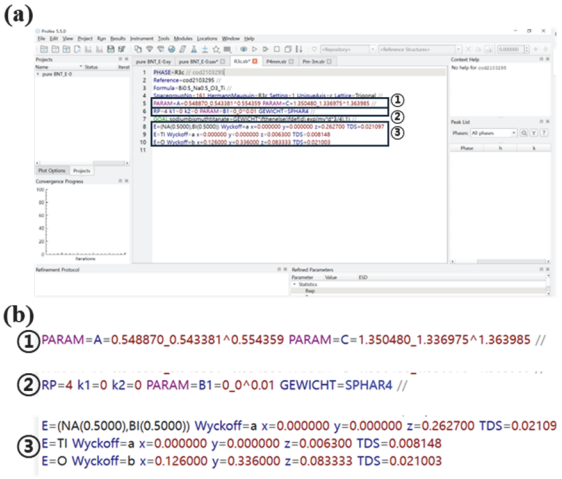

Fig. 24. (a) Screen capture of a window showing the STR files of the Rietveld refinement process and (b) the highlighted areas ①, ②, and ③ in (a) represent the lattice constants; scale factor and thermal vibration factors; and atomic positions and displacements, respectively.

the generated diffraction pattern plots. The refined lattice parameters and phase fractions obtained from the **.lst file include associated uncertainties (± values), which reflect the confidence intervals derived from the least-squares refinement. These deviations should be carefully considered when interpreting structural trends, particularly in multiphase systems or regions near phase boundaries, where small variations can have significant implications, as shown in Fig. 23(b).

- If R_{phase} is much higher than R_{wp}, the refinement fit will not be perfect, and the parameters can be further adjusted until we get comparable values of R_{phase} and R_{wp} (Fig. 24(a) and (b)).

5.7 Saving and Presentation of Rietveld Refinement Results

- Rietveld refinement results can be saved in separate files containing the XRD fitting data for each phase, along with peak positions and phase fraction values.
- The XRD fitting results for each phase can be saved as shown in Fig. 25. When saved, the data is stored in a file with an extension such as "**.xy". This file includes the measured XRD pattern (Y_{obs}), the calculated pattern (Y_{cal}), the difference between the two, the background signal, and the fitting results for each individual phase.

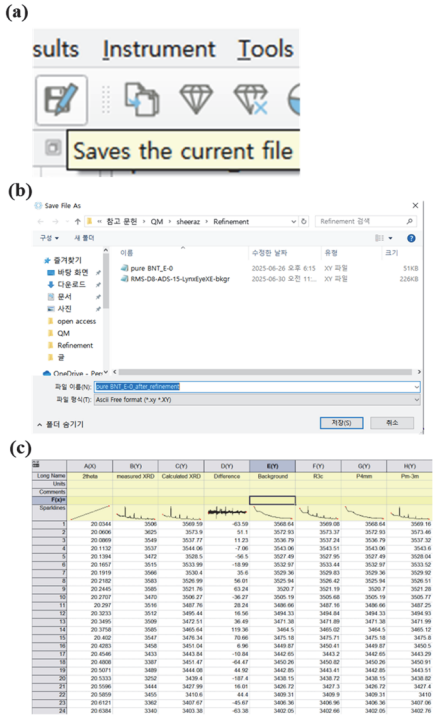

Fig. 25. (a), (b) Screenshot showing the process of saving the final refined file (**.xy) and (c) importing the saved file into ORIGIN for data analysis and visualization.

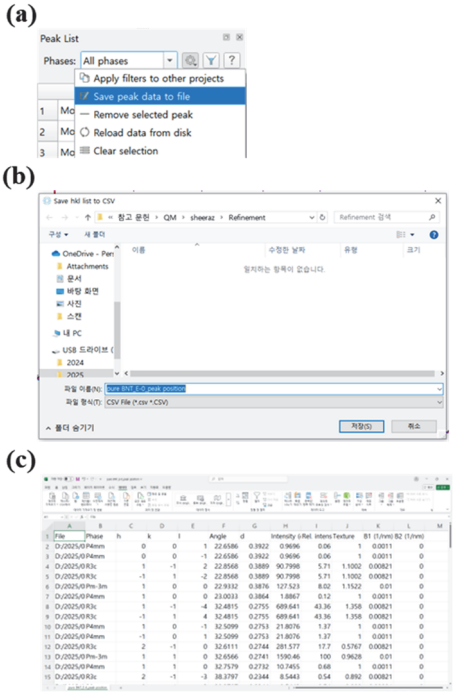

Fig. 26. (a), (b) Screenshot showing the process of saving peak position values from PROFEX and (c) importing the corresponding (**.csv) file into EXCEL for further analysis.

- The peak position values for each phase can be saved as shown in Fig. 26. The data is stored in a file with a ".csv" extension, which includes the Miller indices, peak positions, and intensities for each phase.
- The phase fraction values for each phase can be saved as shown in Fig. 27. When saved, the data is stored in a file with an extension such as "**.csv". This file includes the phase fraction values for each phase and refinement indicators.

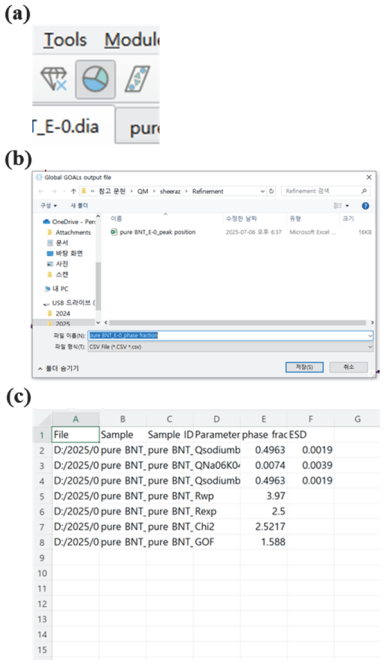

Fig. 27. (a), (b) Screen capture showing the process of saving phase fraction values from the PROFEX program and (c) importing the corresponding (**.csv) file into EXCEL for further analysis.

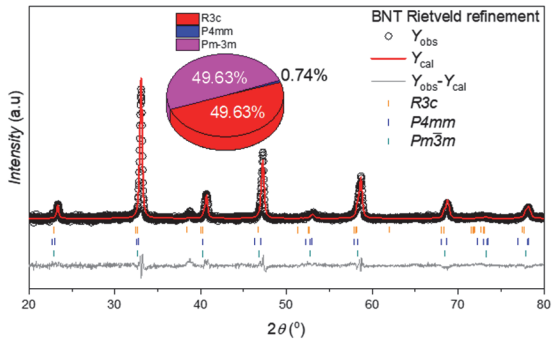

Fig. 28. Example graphs plotted using ORIGIN software based on the Rietveld refinement results.

- The data files containing the XRD fitting results for each phase, along with the peak position and phase fraction values, can be used to generate graphical representations, as illustrated in Fig. 28.

6. ADVANTAGES AND LIMITATIONS OF RIETVELD REFINEMENT

6.1 Advantages: Quantitative Analysis, Multi-phase Systems, and *In situ* XRD Compatibility

- Rietveld refinement offers significant advantages over traditional qualitative XRD analysis by modeling the entire diffraction pattern through mathematical calculations, rather than relying solely on individual peak positions.
- It enables the simultaneous and quantitative extraction of various crystallographic parameters, including lattice constants, phase fractions, and atomic occupancies. This makes it highly effective for analyzing complex multi-phase systems and doped materials.
- Because the refinement parameters carry direct physical meaning, structural responses to experimental variables, such as temperature, electric field, and pressure, can be reflected and interpreted in a meaningful way.
- In recent years, the integration of Rietveld refinement with *in situ* or operando XRD techniques has enabled real-time monitoring of structural changes during electrochemical reactions or under external stimuli. This has expanded its applicability to research areas such as batteries, catalysts, and ferroelectric materials.

6.2 Limitations: Model Dependence, Peak Overlap, and Uncertainty in Complex Systems

- One fundamental limitation of Rietveld refinement lies in its strong dependence on the initial structural model. Since the refinement process calculates the diffraction pattern based on a predefined structure, inaccurate or inappropriate models can lead to poor convergence or distorted results. Therefore, prior knowledge and accurate structural information are essential.
- Severe peak overlaps in the diffraction pattern poses additional challenges, particularly when the sample

contains nano-sized grains or multiple phases with similar symmetries. In such cases, distinguishing between phases and refining individual parameters becomes difficult, increasing the uncertainty of the results.

- When analyzing multi-phase systems, interference among phases and interdependence between refinement parameters can lead to instability in the fitting process. This may result in non-converging refinement or yield physically unrealistic outcomes.
- Please note that PROFEX may not be suitable for systems with severe peak overlap, anisotropic microstrain, or structural disorder due to its simplified peak broadening models. (https://www.profex-xrd.org)

7. CONCLUSION AND OUTLOOK

- This tutorial has provided a comprehensive introduction to the practical procedures, and application cases of Rietveld refinement for the quantitative analysis of crystal structures using X-ray diffraction data. Through hands-on examples using PROFEX software, the study demonstrated how key structural parameters, including lattice constants and phase fractions, can be reliably extracted and interpreted.
- The technique was shown to be particularly powerful for analyzing complex material systems, such as multi-phase ceramics, doped compounds, and materials undergoing structural transitions under external stimuli (e.g., temperature, electric field, chemical environment, and electrochemical cycling). Case studies illustrated how Rietveld refinement facilitates a deeper understanding of structure–property relationships in functional materials
- Looking forward, the integration of Rietveld refinement with *in situ*/operando XRD techniques, and AI-driven automation is expected to significantly enhance its accuracy, throughput, and accessibility. As a result, Rietveld refinement will continue to evolve as a core analytical tool for materials design, functional characterization, and real-time monitoring in a wide range of research and industrial fields.

ORCID

Chang Won Ahn https://orcid.org/0000-0003-0613-9823

ACKNOWLEDGEMENTS

This research was supported by Basic Science Research Program through NRF (RS-2023-00245221) and (RS-2023-00249613).

REFERENCES

[1] J. Y. Park, T. A. Duong, S. S. Lee, C. W. Ahn, B. W. Kim, H. S. Han, and J. S. Lee, *J. Korean Inst. Electr. Electron. Mater. Eng.*, **36**, 513 (2023).
doi: https://doi.org/10.4313/JKEM.2023.36.5.12

[2] S. J. Hyoung, E. S. Kang, Y. Kang, C. R. Kim, C. W. Ahn, B. W. Kim, J. S. Lee, and H. S. Han, *J. Korean Inst. Electr. Electron. Mater. Eng.*, **37**, 433 (2024).
doi: https://doi.org/10.4313/JKEM.2024.37.4.11

[3] T. H. Park, J. W. Moon, T. A. Duong, Y. Kang, H. J. Mun, C. W. Ahn, J. S. Lee, and H. S. Han, *J. Korean Inst. Electr. Electron. Mater. Eng.*, **38**, 448 (2025).
doi: https://doi.org/10.4313/JKEM.2025.38.4.15

[4] H. M. Rietveld, *J. Appl. Crystallogr.*, **2**, 65 (1969).
doi: https://doi.org/10.1107/s0021889869006558

[5] L. Lutterotti and P. Scardi, *J. Appl. Crystallogr.*, **23**, 246 (1990).
doi: https://doi.org/10.1107/S0021889890002382

[6] J. S. Choi, T. H. Kim, and C. W. Ahn, *J. Korean Inst. Electr. Electron. Mater. Eng.*, **35**, 431 (2022).
doi: https://doi.org/10.4313/JKEM.2022.35.5.2

[7] A. Ullah, R. A. Malik, A. Ullah, D. S. Lee, S. J. Jeong, J. S. Lee, I. W. Kim, and C. W. Ahn, *J. Eur. Ceram. Soc.*, **34**, 29 (2014).
doi: https://doi.org/10.1016/j.jeurceramsoc.2013.07.014

[8] S. Ali, M. Sheeraz, A. Ullah, W. S. Yun, A. Ullah, I. W. Kim, and C. W. Ahn, *Chem. Eng. J.*, **485**, 150087 (2024).
doi: https://doi.org/10.1016/j.cej.2024.150087

[9] M. Sheeraz, S. S. Won, J. P. Kim, S. Ali, F. Akram, H. S. Han, B. C. Park, T. H. Kim, I. W. Kim, A. Ullah, and C. W. Ahn, *J. Adv. Ceram.*, **14**, 9221034 (2025).
doi: https://doi.org/10.26599/JAC.2025.9221034

[10] L. de Biasi, A. Schiele, M. Roca-Ayats, G. Garcia, T. Brezesinski, P. Hartmann, and J. Janek, *ChemSusChem*, **12**, 2240 (2019).
doi: https://doi.org/10.1002/cssc.201900032

[11] K. Chen, T. Yan, X. Lei, S. Lanceros-Méndez, Z. Yuan, L. Fang, B. Peng, D. Wang, L. Liu, and Q. Zhang, *J. Am. Ceram. Soc.*, **107**, 4096 (2024).
doi: https://doi.org/10.1111/jace.19705

[12] Y. Huang, C. Zhao, B. Wu, and J. Wu, *J. Am. Ceram. Soc.*, **102**, 2648 (2018).
doi: https://doi.org/10.1111/jace.16139

[13] J. Goetze, I. Yarulina, J. Gascon, F. Kapteijn, and B. M. Weckhuysen, *ACS Catal.*, **8**, 2060 (2018).
doi: https://doi.org/10.1021/acscatal.7b04129
[14] N. U. Khan, W. S. Yun, A. Ullah, S. Ali, M. Sheeraz, A. Ullah, I. W. Kim, and C. W. Ahn, *Ceram. Int.*, **50**, 8790 (2024).
doi: https://doi.org/10.1016/j.ceramint.2023.12.195
[15] M. Sheeraz, B. C. Park, and C. W. Ahn, *J. Korean Inst. Electr. Electron. Mater. Eng.*, **38**, 143 (2025).
doi: https://doi.org/10.4313/JKEM.2025.38.2.3
[16] A. Le Bail, H. Duroy, and J. L. Fourquet, *Mater. Res. Bull.*, **23**, 447 (1988).
doi: https://doi.org/10.1016/0025-5408(88)90019-0
[17] B. H. Toby, *Powder Diffr.*, **21**, 67 (2012).
doi: https://doi.org/10.1154/1.2179804